Talanta 134 (2015) 136–143

Contents lists available at ScienceDirect

Talanta

journal homepage: www.elsevier.com/locate/talanta

Anodic stripping voltammetry of gold nanoparticles at boron-doped diamond electrodes and its application in immunochromatographic strip tests

Tribidasari A. Ivandini [a,b,*], Wiyogo P. Wicaksono [a], Endang Saepudin [a], Bakhadir Rismetov [a], Yasuaki Einaga [b,c,*]

[a] Department of Chemistry, Faculty of Mathematics and Science, University of Indonesia, Kampus UI
[b] Department of Chemistry, Keio University 3-14-1 Hiyoshi, Yokohama 223-8522, Japan
[c] JST-CREST, 3–14-1 Hiyoshi, Yokohama 223–8522, Japan

ARTICLE INFO

Article history:
Received 9 August 2014
Received in revised form
4 November 2014
Accepted 5 November 2014
Available online 13 November 2014

Keywords:
Melamine
Anodic stripping voltammetry
Gold nanoparticles
Boron-doped diamond electrode
Immunochromatographic strip tests

ABSTRACT

Anodic stripping voltammetry (ASV) of colloidal gold-nanoparticles (AuNPs) was investigated at boron-doped diamond (BDD) electrodes in 50 mM $HClO_4$. A deposition time of 300 s at −0.2 V (vs. Ag/AgCl) was fixed as the condition for the ASV. The voltammograms showed oxidation peaks that could be attributed to the oxidation of gold. These oxidation peaks were then investigated for potential application in immunochromatographic strip tests for the selective and quantitative detection of melamine, in which AuNPs were used as the label for the antibody of melamine. Linear regression of the oxidation peak currents appeared in the concentration range from 0.05–0.6 μg/mL melamine standard, with an estimated LOD of 0.069 μg/mL and an average relative standard deviation of 8.0%. This indicated that the method could be considered as an alternative method for selective and quantitative immunochromatographic applications. The validity was examined by the measurements of melamine injected into milk samples, which showed good recovery percentages during the measurements.

1. Introduction

In recent years, metal nanoparticles have gained considerable attention as labels in analytical methods based on affinity reactions, such as immunosensors and immunoassays [1–5]. In particular, immunochromatographic strip tests, which combine chromatographic techniques with immunoreactions, offer wide applications in protein analysis and clinical diagnosis [5–11]. Among many types of metal nanoparticles, gold nanoparticles (AuNPs) have been the most extensively studied due to their unique optical, chemical, electrical, and catalytic properties[12]. In addition, AuNPs can provide good affinity for covalent bonds with proteins[12] . Based on these properties, the application of AuNPs for immunochromatographic strip tests has been reported [7–11]. Furthermore, although qualitative detections using immunochromatographic techniques offer selectivity, simplicity, and versatility [5–10], quantitative determination is also required [10–12]. Optical methods were generally incorporated to quantify the AuNP labels in immunochromatography [5–9]. However, the optical methods have limited applicability due to optical interference as well as the liquids that are used as solvents.

On the other hand, boron-doped diamond (BDD) electrodes are superior to other conventional solid electrodes due to their wide potential window, very low charging current, chemical inertness, mechanical durability, and good biocompatibility [13–15]. Electrochemical applications using BDD electrodes have been reported for many types of chemicals and biochemical sensors [13–20], including metals and heavy metals sensors [14,16–20]. Accordingly, anodic stripping voltammetry (ASV) is generally considered as the most suitable method for trace-level metal detections since the method offers several advantages for metal analysis, including high selectivity and sensitivity, low detection limits, simple operation, and economical cost [16–20]. Since ASV involves deposition and stripping processes at the working electrodes, the inert surfaces of BDD electrodes make a significant contribution in that they provide better stability in comparison to other solid electrodes [16–20]. Furthermore, ASV of AuNPs in immunochromatographic strip test applications has already been reported using carbon paste electrodes [10,11]. However, because the presence of proteins causes fouling of the electrodes, a disposable system was suggested not only for the strip tests but also for the working electrodes [10,11].

In this work, ASV of AuNPs at BDD electrodes was studied. $HClO_4$ was found to be the most suitable supporting electrolyte. It was also found that after an initial coating of gold had been

* Corresponding authors.
E-mail address: einaga@chem.keio.ac.jp (Y. Einaga).

http://dx.doi.org/10.1016/j.talanta.2014.11.010
0039-9140/

deposited at the BDD surface, a new peak at around −0.1 V that is attributable to the formation of Au_2O_3 could be observed. As a model for further applications, the method was combined with immunochromatographic strip tests for the quantitative detection of melamine. Melamine is a synthetic compound that is used as an industrial chemical for the production of plastics, amino resins, and flame retardant materials [21–23]. However, it was recently found that melamine has been deliberately added to milk and to cheese [23,24]. Since the conventional detection method for proteins (Kjehldahl method) only determines the nitrogen content, the presence of melamine can create a false indication regarding the protein content. Various analytical methods have been developed for the detection of melamine, such as chromatography [8,23–25], capillary electrophoresis [11], and enzyme-linked immunosorbent assay (ELISA) [12], which require expensive instruments as well as highly skilled operators. Therefore, a rapid, sensitive, and inexpensive detection method for melamine is definitely necessary [7]. The melamine strip test was prepared with reference to the earlier reports, based on the complex reaction between melamine and the antibody of melamine (anti-melamine) [10,11,23,26]. AuNP was used for the label for anti-melamine and the detection of melamine was performed based on the assumption that the quantity of AuNPs involved in the system was equivalent to the concentrations of the antibody and of melamine [10,11]. The utilization of BDD for ASV measurements of AuNPs was demonstrated to provide a quantitative detection of melamine using immunochromatographic strip tests. The stability of BDD electrodes enabled a low limit of detection (LOD) and a good stability of the current responses to be achieved. Moreover, good percentage recovery of the measurements in milk sample matrices was shown, indicating that the method is promising for applications in immunochromatographic strip tests with metal nanoparticle labels.

2. Experimental

2.1. Chemicals and materials

Melamine, trisodium citrate, hydrogen tetracholoroaurate (III) tetrahydrate, perchloric acid, trimethoxyborane, and other chemicals were supplied from Wako. Bovine serum albumin (BSA), millipore glass-fiber filters AP2002500 (borosilicate with an acrylic binder suitable to protect a 0.8–8 μm membrane), and a nitrocellulose membrane with a pore size of 5 μm was purchased from Sigma Aldrich. Melamine antibody (polyclonal antibody of melamine, anti-melamine, 500 μg/L) was obtained from Beacon. Silicon wafers were purchased from Mitsubishi Metal Corp. Plastic backing and a liquid blocker super pap pen mini were supplied by Cosmo Bio (Japan).

2.2. Electrode preparation.

The BDD electrode was prepared using microwave plasma-assisted chemical-vapor deposition (MPACVD) (ASTeX Corp.), and a mixture of 50 mL of acetone and 4 mL of trimethoxyborane was used to provide sources of carbon and boron, respectively. Details of the preparation procedure are described elsewhere [13]. Scanning electron microscopy (SEM) showed that the grain sizes of the polycrystalline film were ~2–5 μm with 5 μm thickness. Characterization with Raman spectroscopy (Renishaw System 2000) provided a typical spectrum with a peak at 1333 cm^{-1} related to sp^3 carbon bonds and a couple of peaks at ~500 and 1200 cm^{-1} that confirmed the existence of boron doping in the diamond structure [13,27,28]. The absence of a peak at ~1600 cm^{-1}, which is generally attributed to 'non-diamond' carbon, suggested that the BDD thin films were of fine quality [13,27,28].

2.3. Preparation of AuNPs and AuNPs-modified anti-melamine (AuNP-antimel)

AuNP was synthesized by boiling 100 mL of 0.01% $HAuCl_4$ solution with constant stirring. Then, 2.0 mL of 1% trisodium citrate was added into the solution and the boiling process was continued for 15 min. After cooling to room temperature, the volume of the colloidal AuNPs was readjusted using deionized water. In order to prepare AuNP-antimel, 10 mL of colloidal AuNPs was adjusted to pH 7 using 0.1 M K_2CO_3 before carefully adding 0.5 mL of antimel (0.1 mg/mL). After incubation was completed, 3 mL of 5% BSA was added followed by further incubation. The incubation time of AuNP-antimel was monitored using the adsorption peak of AuNPs at ~520 nm by UV-visible spectroscopy. The solution was then centrifuged at 180,000 rpm for 30 min. The red precipitate was rinsed as a re-suspension in 2 mL 0.01 mL of phosphate buffer solution (PBS) containing 5% sucrose, 5% BSA, and 0.4% Tween-20 pH 7.4 and kept in storage at 4 °C when not in use. TEM, UV–vis and FT-IR spectroscopy were used to characterize the AuNPs and the AuNP-antimel.

2.4. Fabrication of immunochromatographic strip test [23,26]

The immunochromatographic strip test was assembled from several components, including a sample pad, a conjugate pad, a nitrocellulose membrane, a capturing antibody pad/test zone, a control line pad, and an absorbent pad. All of the components were arranged on a plastic backing sheet as shown in Fig. 1. The sample, the conjugate, and the absorbent pads were made of

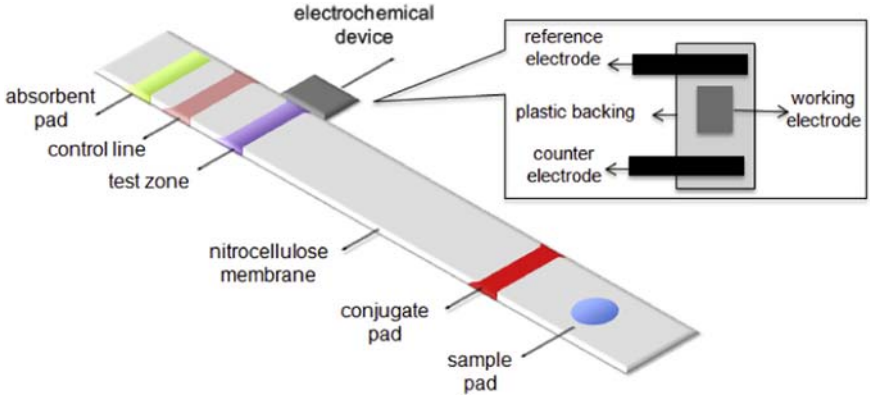

Fig. 1. Scheme of the immunochromatographic strip test. Inset shows the scheme of the electrochemical device.

glass-fiber filter material, whereas the test zone and the immunochromatographic reaction zone were prepared using a nitrocellulose membrane. The conjugate pad was prepared by carefully dropping 100 μL of AuNP-antimel followed by drying at room temperature. The procedure was repeated twice. Meanwhile, the capturing antibody and the control line pads were prepared by the same method each using 100 μL of 5% anti-melamine and 100 μL of 5% goat-anti mouse IgG, respectively, in 0.02 M PBS at pH 7.4. The electrochemical device consisted of a BDD film (4 mm × 4 mm), a Pt wire (Nilaco Japan), and an Ag/AgCl system as the working, supporting, and reference electrodes, respectively. All of the electrodes were assembled into an electrochemical cell on a plastic backing (inset of Fig. 1).

2.5. Immunochromatographic strip test coupled with electrochemical detection

The immunochromatographic strip test coupled with electrochemical detection was evaluated using standard solutions of melamine. A 100 μL sample of the solution was introduced onto the sample pad. The sample moved through the conjugate pad and the nitrocellulose membrane, respectively, toward the test zone. After ~7 min immunoreaction, the test zone was blocked with two lines drawn by a liquid blocker pen with a distance of ~10 mm between the lines. Then, 200 μL of 0.05 M $HClO_4$ was dropped in the test zone as the supporting electrolyte and electrochemical measurements were conducted using the ASV technique with a galvanostat (ALS CHI BAS).

3. Results and discussion

3.1. Preparation of AuNPs and AuNP-antimel

The AuNPs were synthesized as a ruby red colloidal solution. The TEM image in Fig. 2(a) shows that the AuNPs have an average diameter of ~17 nm and that noticeable clusters form with a uniform size, indicating that the citrate used as a reducing agent can also act as a capping agent (stabilizer) [29]. The AuNPs were then introduced into anti-melamine to form AuNP-antimel. Antibodies, including anti melamine, are a type of protein containing many N atoms and possibly some S atoms. The affinity of N or S atoms to AuNPs is known to be higher than O or C atoms in citrate molecules. Therefore, anti-melamine can theoretically interact more strongly with AuNPs than with citrate molecules and easily replaces the position of the citrate as the capping agent. Observations using the UV-visible spectra of AuNPs in Fig. 2(b) shows an absorbance wavelength at ~520 nm. The absorbance decreased after the addition of anti-melamine. The decrease reached a

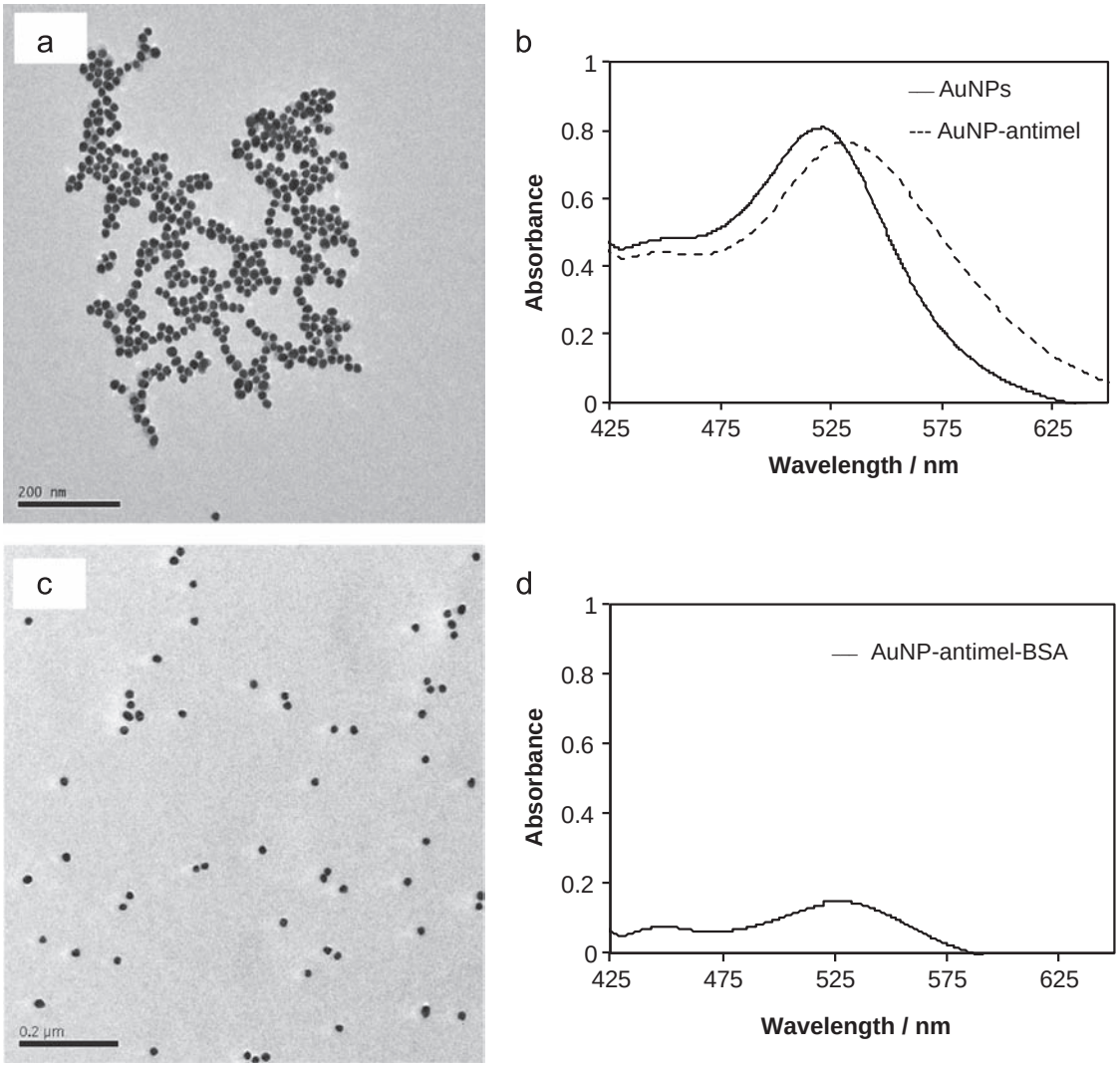

Fig. 2. TEM Images and UV–vis spectra of AuNPs (a and b, respectively) in the absence, and (c and d, respectively) in the presence of anti-melamine and 5% BSA.

maximum after 10 min indicating that the interaction between AuNPs and anti-melamine was complete.

Furthermore, BSA needed to be added in order to enable interaction between the active site of the antibodies (paratope) with the antigens (melamine) at the epitope site [30]. BSA, which consists of amino acid sequences, is expected to fill the end of the "Y" antibody (antigen binding site). As a result, the antibody is expected to be able to specifically recognize and bind with melamine [10,11,26]. In this work a polyclonal antibody was employed. Polyclonal antibody has the disadvantage compared with monoclonal antibody, in terms of specificity and selectivity. However, since in this method immunosensor and the chromatographic paper were combined, the selectivity was expected to increase. The TEM image in Fig. 2(c) shows that the diameter of the AuNPs was not affected when the AuNPs were conjugated or labeled to antibodies in the presence of BSA. However, the distance between the AuNPs increased, indicating that the AuNP was surrounded by antibodies with large molecular sizes and by BSA. The UV–vis spectra, shown in Fig. 2(b) and (d) also confirmed that although the peak intensity was decreased, a very slight chemical shift occurred at the absorbance peak of AuNP-antimel compared with that of AuNPs, suggesting that the AuNPs were stable despite conjugation with the antibodies.

In order to confirm the interaction between AuNPs and anti-melamine-BSA, characterization was also performed using IR spectroscopy on AuNPs, anti-melamine, and AuNP-antimel (Fig. 3 (a)). Before the measurements, centrifugation was conducted to reduce the influence of water. The two sharp peaks that appeared at the wavenumbers of 3300 cm^{-1} and 1645 cm^{-1} in all of the spectra confirmed the presence of O-H and C=O bonds, respectively, which are normally available when AuNPs are stabilized by citrate functional groups, and the antibody also contains some OH and C=O functional groups. In the fingerprint region at 900–1500 cm^{-1} shown in Fig. 3(b) and (c), no clear peak appeared in the spectrum of AuNPs. However, some strong and weak peaks were observed in the spectra of anti-melamine and AuNP-antimel, such as those at wavenumbers 995, 1050, 1085 cm^{-1}, which are related to the absorption of N-H, C=S, and N=O, respectively. These peaks confirmed the presence of protein (anti melamine and BSA). The absence of any new peak and the decrease in all peak transmittance in the spectrum of AuNP-antimel indicated there were no bonds formed between AuNPs and anti-melamine, confirming that the AuNPs could only be wrapped by the large molecular sizes of the antibodies and BSA.

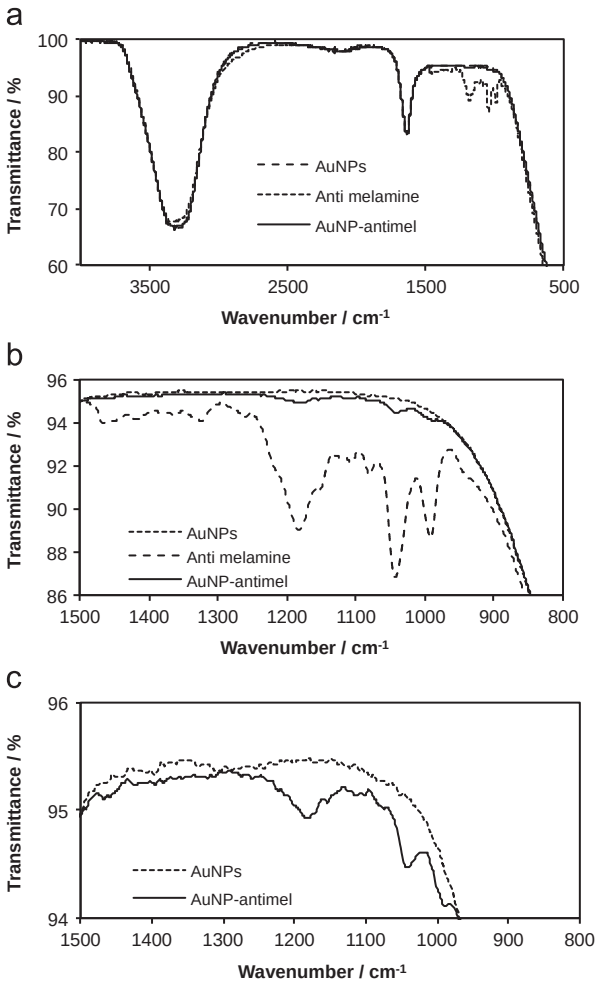

Fig. 3. IR spectra of AuNPs, anti-melamine, and AuNP-antimel (a) with their fingerprint region zoomed in (b) for all spectra and (c) for AuNPs and AuNP-antimel spectra.

3.2. Anodic stripping voltammetry of AuNPs

In order to quantify the AuNPs, the ASV technique was applied. Voltammograms of AuNPs in four different types of electrolytes are shown in Fig. 4. The electrolyte was used not only to maintain the ionic strength of the electrochemical system, but also for the dissolution of the AuNPs to gold ions. When using the ASV technique, the gold ions are expected to be electrochemically concentrated as Au^0 at the surface of the BDD electrodes. Therefore, when the stripping process to a higher potential is conducted, a high oxidation peak for Au^0, which is attributable to the concentration of AuNPs, can be expected. Fig. 4(a) shows the voltammograms recorded over the potential range from −0.5 V to 1.5 V with a deposition time of 60 s and a scan rate of 100 mV/s. A well-defined peak at a potential of +0.7 V (vs. Ag/AgCl) was obtained when the electrolyte was 50 mM PBS at pH 7.4. However, when the electrolyte was substituted with 50 mM HCl, the peak shifted to +1.1 V (Fig. 4(b)). This peak presented a sharper peak-shape with higher oxidation current. Typical results were also obtained when the electrolytes were substituted with 50 mM H_2SO_4 or 50 mM $HClO_4$ as shown in Fig. 4(c) and (d), respectively. The data suggested the influence of pH on the ASV of AuNPs. More detailed experiments regarding the pH dependence issue confirmed the dependence of the oxidation potential peak of ASV on the pH condition with dE/dpH ~57 mV, which was indicative of a for the mechanism where equal numbers of electrons and protons are involved. The data is also in agreement with the potentials-pH equilibrium diagram of gold, which showed a decrease in peak potentials as the pH increased [32].

Furthermore, the voltammogram of AuNPs in $HClO_4$ showed a higher signal-to-background ratio compared to those in HCl or in H_2SO_4. It seems that the properties of $HClO_4$ as a strong acid (pKa = −10) as well as a strong oxidizing agent cause better dissolution of AuNPs to gold ions. As a consequence, $HClO_4$ was selected as the electrolyte in the next experiments.

When the same experiments were performed using a 10 mM $HAuCl_4$ solution, they showed typical voltammograms, confirming that the same reduction-oxidation reaction has occurred. Meanwhile, experiments performed using glassy carbon electrodes with AuNPs also provided typical voltammograms with the stripping peak shifted to a more negative potential at +1.0 V (data not shown). This shifting is reasonable, since the sp^3 coordination of the BDD surface generally causes slower kinetics of the oxidation/reduction reaction than an sp^2 surface such as a glassy carbon electrode [13]. However, because glassy carbon provided more adsorption on its surface than BDD, it was difficult to get stable peak currents at glassy carbon electrodes. Typical oxidation potentials were also shown in the ASV of $HAuCl_4$ in

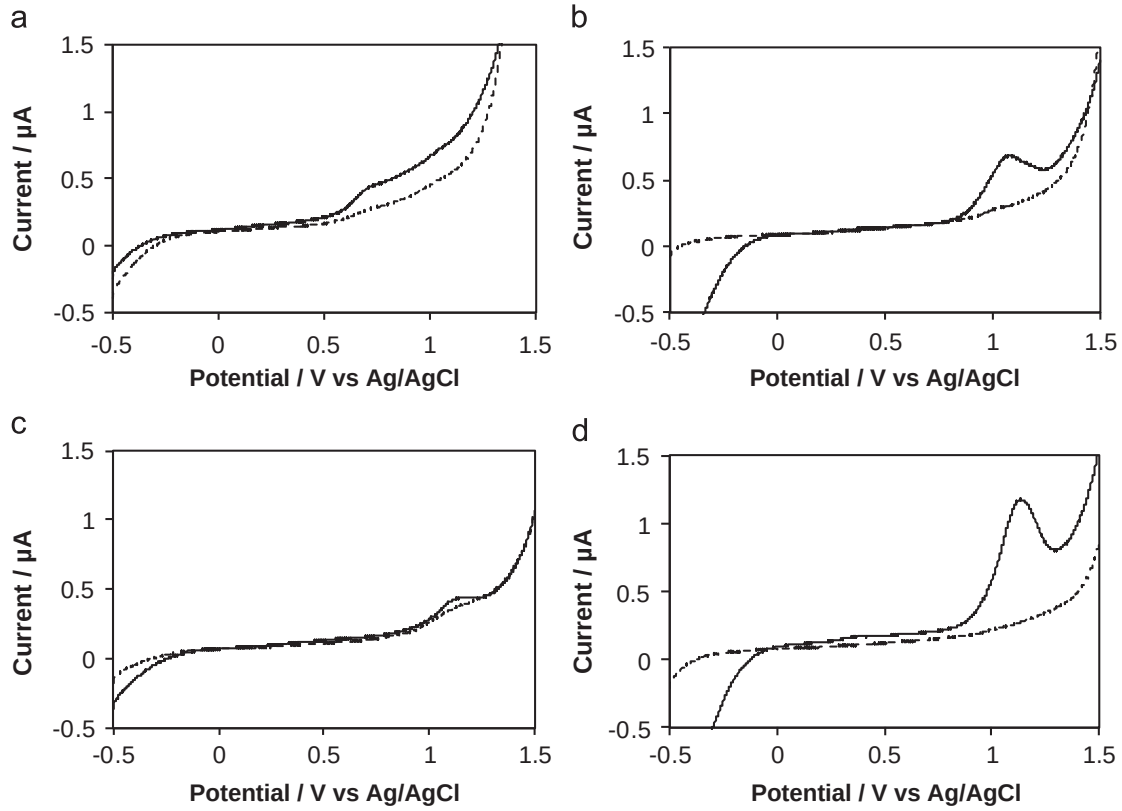

Fig. 4. Anodic stripping voltammograms of (a) 50 mM phosphate buffer pH 7, (b) 50 mM HCl, (c), 50 mM H_2SO_4, and (d) 50 mM $HClO_4$ in the absence (dotted line) and in the presence (solid line) of 50% AuNPs (v/v) measured using BDD electrodes as the working electrodes. Deposition potential was −0.5 V, deposition time was 60 s, and scan rate was 100 mV/s.

a mixed solution of HCl/HNO_3 at glassy carbon electrodes [31], indicating that a similar reduction oxidation reaction of AuNPs occurred as to that of $HAuCl_4$, as follows [31,32],

$$\text{Deposition step } [AuCl_4]^- + 3e^- \rightarrow Au + 4\ Cl^- \quad (1)$$

$$\text{Stripping step } Au + 3H_2O \rightarrow HAuO_3 + 3H^+ + 3e^- \quad (2)$$

Investigation of various deposition times was conducted, starting from 60 s to 300 s. As expected, the increase of the deposition time leads to a higher peak current at +1.1 V, as shown in Fig. 5. The current continues to increase with deposition time until it reaches 300 s. Therefore, to limit the time required for the measurements, a deposition time of 300 s was applied as the deposition time for the rest of the experiments. However, in addition to the peak at +1.1 V, another oxidation peak at −0.1 V appeared when the deposition time started from 180 s. The peak current also became higher as the deposition time increased. Interestingly, once the peak appeared, it remained observable although the deposition time decreased to less than 180 s. Since the peak at +1.1 V can be attributed to the oxidation of Au^0 to Au^{3+} and the peak at −0.1 V appeared after relatively high intensity of deposited Au^0, it is reasonable to correlate the peak to the oxidation of Au^0 to Au_2O_3, which was formed from gold particles deposited at the surface of the BDD as follows [32]:

$$2Au + 3H_2O \rightarrow Au_2O_3 + 6H^+ + 6e^- \quad (3)$$

Basically, BDD with sp^3 coordination is known to have physically- and chemically-stable surfaces due to its sp^3 bonds [13]. These characteristics indicate that the deposition of metal onto a BDD surface is difficult to achieve. Uchikado et. al reported that it is necessary to change the surface of BDD from H- to O-termination to increase the affinity of the surface to metal particles [33]. Other reports showed the requirements to modify the surface of BDD using a photochemical reaction before gold nanoparticles attached at the surface [34,35]. However, once the nucleation has started at the surface, it becomes easier to deposit more gold on the small gold particles that have already deposited. It seems that a minimum amount of deposited gold is required to allow the formation of Au_2O_3, and therefore, this peak was not observable in several of the initial voltammograms shown in Fig. 4(d) and Fig. 5(a). In addition to the increase in peak current at −0.1 V and +1.1 V against the deposition time, increase in the baseline currents of the voltammograms was also observed (Fig. 5(a)), which is reasonable since some small particles of gold remained at the surface of the BDD that then acted as 'gold-microarray modified' BDD electrodes [36].

Applying a deposition time of 300 s with various deposition potentials from −0.5 V to −0.2 V showed that both oxidation peak currents at −0.1 V and +1.1 V increased, then decreased as a more positive potential was applied (Fig. 5(c)). Based on this result, the deposition potential for the rest of the experiments was fixed at −0.2 V.

Both oxidation peaks were then investigated using the ASV technique for various concentrations of AuNPs dissolved in 50 mM $HClO_4$. Fig. 6(a) shows that an increase in the AuNP concentration leads to peak currents, not only for the peak at +1.1 V but also for the peak at −0.1 V. The linear calibration curves of the peak currents displayed in Fig. 6(b) shows that the currents of both peaks were linear with respect to AuNP concentrations in the concentration range from 10% to 50% of colloidal AuNPs or equivalent to 0.01 ppm to 0.05 ppm (R^2 of 0.99 and 0.98) for the peaks at −0.1 V and +1.1 V, respectively. The limits of detections (LODs) were estimated to be 0.0067 and 0.0077 ppm Au or equivalent to 34 nM and 39 nM, respectively, for the peaks at

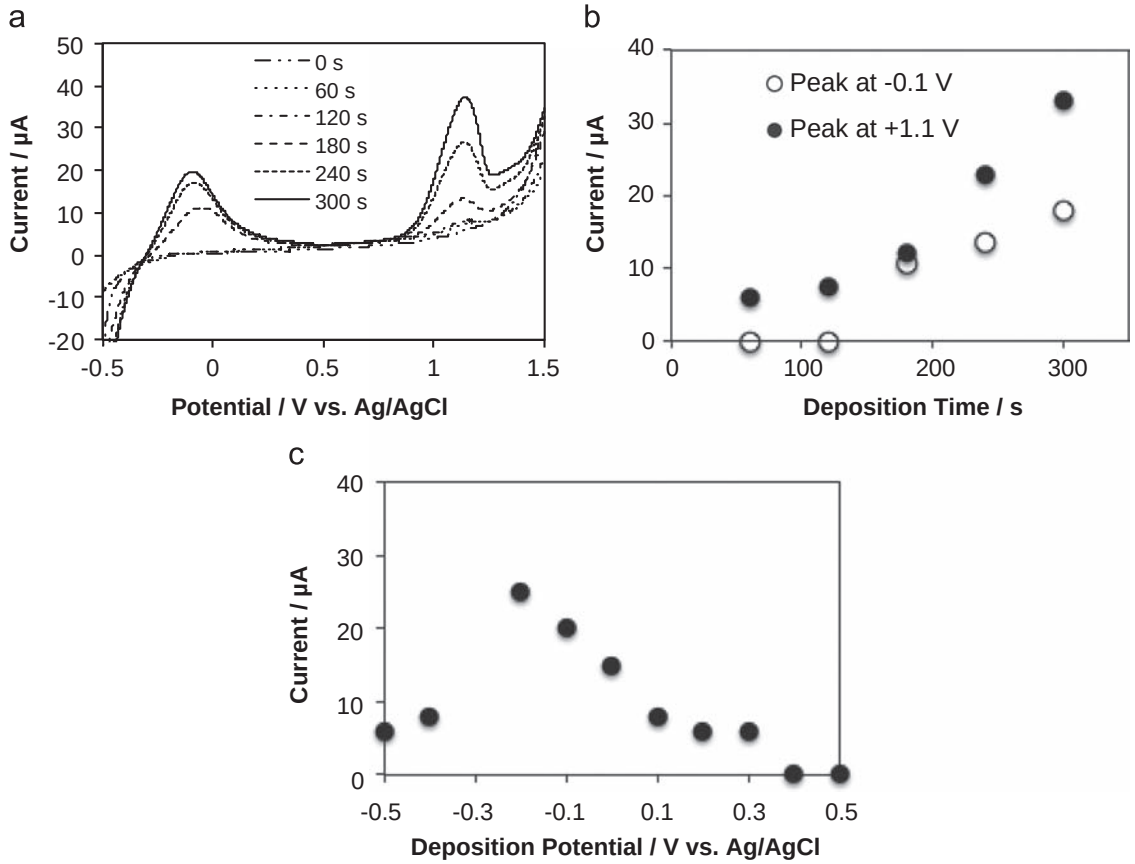

Fig. 5. (a) Anodic stripping voltammograms of 50% colloidal AuNPs in 50 mM $HClO_4$ at various deposition times, and (b) the dependence of oxidation peak currents on the deposition times. Data in (b) were extracted from oxidation peaks at −0.1 and +1.1 V. Other conditions were similar to those in Fig. 4.

−0.1 V and +1.1 V. This result was comparable to those of stripping voltammetry at various carbon electrodes, as summarized in Table 1 [37–41]. Although some of the detection methods displayed in Table 1 showed better LODs, one method which employed Br_2 gas is not easy to control [38,39], whereas another method applied the differential pulse voltammetry (DPV) technique, which is generally known to give a better LOD. Since in this method normal ASV is applied, it is estimated that combining ASV with the DPV technique can improve the LOD [34].

Small relative standard deviations (RSD) of 2.42% and 2.59% ($n=3$) were achieved for the current peaks at −0.1 V and +1.1 V, respectively, indicating that the current responses were quite stable. A slight increase in the baseline with increasing deposition time, as observed in Fig. 6(a), suggested that a small amount of gold might be remained at the surface of the BDD and confirmed the contribution of the gold-modified BDD in the peak performance at −0.1 V. In order to recover the electrode surface, oxidation at a potential of +3.0 V for 20 min can perfectly strip the gold particles that are deposited at the BDD surface, which is a clear advantage for the use of BDD compared to other types of conventional electrodes [42]. Since both peaks at −0.1 V and +1.1 V exhibit similar performances, both peaks are applicable for the detection of AuNPs.

3.3. Application in immunochromatographic strip test for melamine detection

As a model of application, the ASV method was then utilized for the electrochemical measurement of melamine after separation using the immunochromatographic strip test. When a melamine standard was dropped onto the sample pad, melamine molecules moved by the capillary action of the nitrocellulose membrane to the conjugated pad, in which AuNP-antimel had been immobilized. In the presence of melamine, the interaction of melamine with AuNP-antimel forms a melamine-antibody-gold nanoparticle complex (mel-antimel-AuNP), which continuously moves toward the nitrocellulose membrane and is captured by the antibodies that are immobilized in the test zone to form a sandwich-like antimel-melamine-antimel-AuNP complex. Meanwhile, the AuNP-antimel, which is expected to move forward faster in the absence of melamine, reaches the control line, and arrives at the absorbance pad earlier due to its smaller size than the sandwich complex. The whole movement process from the sample pad to the absorbent pad takes ~7 min, which could be easily monitored from the movement of the pink color of the AuNPs. As a matter of fact, some melamine-antibody complex also reached the control line during this time. However, as shown in the next paragraphs, a linear calibration curve can be achieved for melamine detections by dissolving AuNPs at the detection line.

After the dissolution of the test zone using $HClO_4$, the AuNPs were expected to dissolve as $[AuCl_4]^-$ ions. Therefore, stripping voltammetry could be performed. Volumes of 50, 100, 150 and 200 µL were used to dissolve AuNPs in the test zone of the immunochromatographic strip tests that were employed for 0.5 ppm standard samples of melamine. The anodic stripping voltammograms showed that the peak currents increased for the sample volumes from 50 to 100 µL and reached a maximum from 100 to 200 µL. Therefore, a volume of 100 µL $HClO_4$ was used to dissolve AuNPs in the test zone.

Voltammograms of the developed immunochromatographic strip tests were then performed for a various melamine concentrations (Fig. 7). Fig. 7(a) shows that when melamine was present

in the system, three oxidation peaks were obtained at +0.1 V, +0.4 V and +0.9 V, which were quite different from the peaks in the voltammograms of AuNPs without the strip test (Fig. 6). A possible reason is that peaks at +0.4 V and +0.9 V are due to the presence of melamine in the test zone, which leads to the existence of melamine antibody and BSA besides gold and citrate ions from the AuNPs. Although citrate ions are not electroactive, BSA is reported to be electroactive at BDD electrodes [43]. Previously, we have reported the direct electrochemical oxidation of BSA at pH 7 using bare BDD electrodes, in which cysteine oxidation peaks were observed at around +0.4 V and +0.9 V [41]. Therefore, it is reasonable to presume that those peaks at +0.4 V and +0.9 V are related to the oxidation of cysteine amino acid as a component in BSA or melamine antibody.

Furthermore, shifting of the peaks to more positive potentials was observed from -0.1 V to +0.1 V, while the peak at +1.1 V was at a potential of +1.3 V. This shifting was probably due to an increase of the system viscosity in the presence of BSA and anti-melamine, which affects the reaction kinetics at the electrode surface. Moreover, the position of the electrode under the nitrocellulose membrane (the other site of the reactant) can also affect the mass transfer of the reactant. However, the peak that was observed at +1.3 V was very weak (Fig. 7(a)). Since this peak is attributed to the reaction of solid Au_2O_3 to Au^{3+} [32], it is reasonable that very slow kinetics occurred due to the high

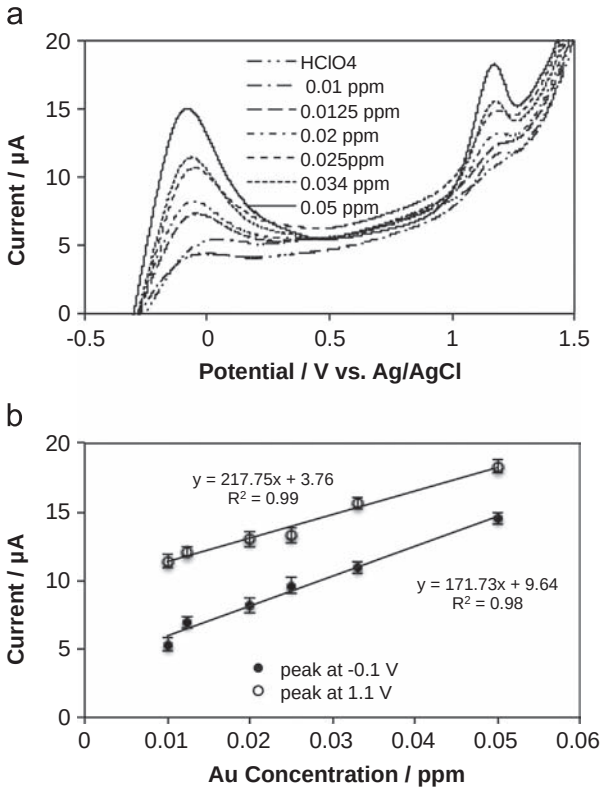

Fig. 6. (a) Anodic stripping voltammograms of various concentrations of AuNPs dissolved in 50 mM $HClO_4$ and (b) the dependence of the oxidation peak currents on the concentration. Data in (b) was extracted from oxidation peaks at −0.1 V (empty circle) and +1.1 V (filed circle) in (a). Deposition potential was −0.2 V, deposition time was 300 s, and scan rate was 100 mV/s.

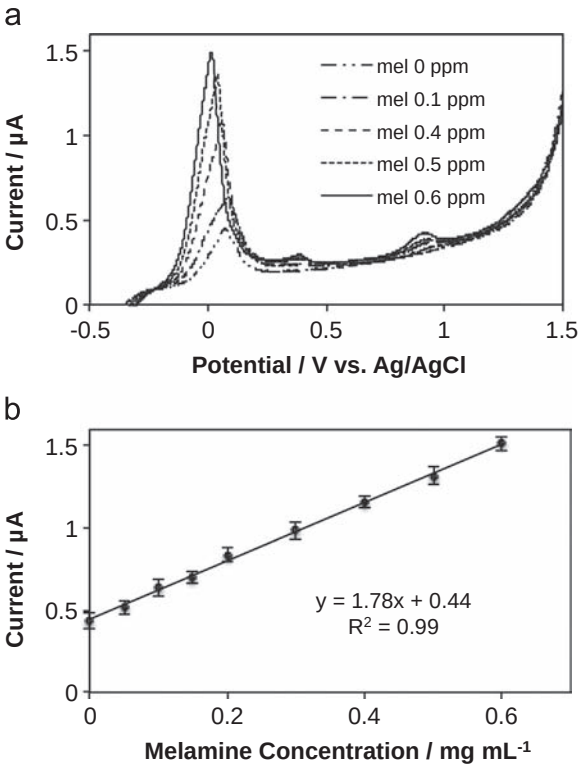

Fig. 7. Anodic stripping voltammograms of antimel-mel-antimel-AuNP complex dissolved in 50 mM $HClO_4$ and obtained from strip tests for various concentrations of melamine (a) and the oxidation peak current dependence on melamine concentrations (b). Data in (b) were extracted from the oxidation peak at ca. 0.0 V (vs. Ag/AgCl) in (a). Other conditions were similar to those of Fig. 6.

Table 2
Comparison of the performance of several detection methods for AuNPs applied in immunochromatographic strip tests for melamine detection.

Sample	Method	LOD
Milk	Optical reader[10]	4.47×10^{-3} µg/mL
Milk	Spectrophotometer[44]	2 µg/mL
Milk	Test-strip reader[45]	260 µg/mL
Milk	This method	0.069 µg/mL

Table 3
Results of strip test in raw milk sample injected by 5.0 µg/mL melamine over 3 measurements.

Injected Melamine (µg/mL)	Strip test ($n=3$) (µg/mL)	GC–MS ($n=3$) (µg/mL)
5.0	4.8 ± 0.4	4.8 ± 0.5
5.0	4.5 ± 0.4	4.8 ± 0.4
5.0	5.8 ± 0.5	5.5 ± 0.3

Table 1
Comparison of the electrochemical methods reported for the determination of gold nanoparticles at various carbon electrodes.

Method	Electrode	Electrolyte	LOD
Differential Pulse Adsorptive Stripping Voltammetry[34]	Graphite	HCl	17.8 nM
ASV[38]	SPE	HBr/Br_2	36 nM
ASV[39]	SPE	HBr/Br_2	5 nM
ASV[40]	Carbon Paste	$NH_3/AgNO_3$	1.8×10^7 gold particle/cm^3
This method	BDD	$HClO_4$	34 nM

viscosity of the system. A control experiment performed with the absence of melamine shows only one oxidation peak at 0.05 V (Fig. 7(a)). The absence of oxidation peak at +0.4 V and +0.9 V was expected since without melamine the AuNP-antimel and BSA would not stop in the test zone, whereas the oxidation peak that appeared at around 0.05 V was assumed to be due to the nonspecific adsorption of some amount of AuNPs, which remains at the membrane during the migration.

Further, while the current peaks at +0.4 V are too low to be analyzed, the peak currents at ca. 0.0 V show a linear dependence over the melamine concentration range from 0.0.5 to 0.6 μg/mL (Fig. 7(b). Linearity of the peak current at +0.9 V was also observed. However, much higher sensitivity was shown by the peak at ca. 0.0 V than at +0.9 V, with an estimated LODs of 0.069 μg/mL and 0.120 μg/mL, respectively. Comparison of this method against the other methods that are applied for immunochromatographic strip tests showed a better LOD than most other reports as summarized in Table 2 [10,44,45]. Moreover, average RSDs of 8.0% and 11.0% were obtained (n=3) for the oxidation peaks at ca. 0.0 V than +0.9 V, respectively, for the melamine concentration range between 0.05–0.6 μg/mL, indicating that the peak at ca. 0.0 V is more suitable for the detection using strip tests. Validation for standard melamine injected into milk samples was conducted using GC–MS and showed similar recovery percentages as shown in Table 3, suggesting that the method can be applied as an alternative detection method after immunochromatographic strip test separation.

4. Conclusion

Boron-doped diamond electrodes were successfully utilized for the detection of gold-nanoparticles (AuNPs) using anodic stripping voltammetry (ASV) with 50 mM $HClO_4$ as the supporting electrolyte. Investigation of the voltammograms with a deposition time of 300 s and a potential deposition of -0.2 V showed linearity for oxidation peak currents at −0.1 V and +1.1 V in the concentration range of 0.01–0.05 ppm of gold, with an estimated limit of detection (S/N=3) of 6.7 ppb (~34 nM). Application of the method for the immunochromatograpic strip tests of melamine showed that the first oxidation peak encountered less interference than the subsequent peaks. Moreover, higher sensitivity of the peak was also shown. The peak response was linear in the concentration range from 0.05–0.6 μg/mL melamine, with limit of detection of 0.069 μg/mL (0.54 μM). Good stability of the current responses suggests that ASV using BDD electrodes can be applied as an alternative non-disposable detector for the quantitative detection using immunochromatographic strip tests.

Acknowledgments

This work was partly granted by Hibah Riset Utama Universitas Indonesia (RUUI) 2013 (DAMAS) Grant No. 0974/H2.R12/HKP.05.00/2013.

References

[1] F.J. Hayes, H.B. Halsall, W.R. Heineman, Anal. Chem. 166 (1994) 1860–1865.
[2] J. Wang, B. Tian, K.R. Rogers, Anal. Chem. 79 (1998) 1682–1685.
[3] J. Wang, Electroanal 19 (2007) 769–776.
[4] M.T. Castaneda, S. Alegret, A. Merkoci, Electroanal 19 (2007) 743–753.
[5] M.G. Weller, J., Fresen, Anal. Chem 266 (2000) 635–645.
[6] Y-Y. Lin, J. Wang, G. Liu, H. Wu, C.M. Wai, Y. Lin, Biosens. Bielectron 23 (2008) 1659–1665.
[7] X. Li, P. Luo, S.S. Tang, R.C. Beier, X.P. Wu, L.L. Yang, Y.W. Li, X.L. Xiao, J. Agric. Food Chem. 59 (2011) 6064–6070.
[8] R.C. Wong, H.Y. Tse, Lateral Flow Immunoassay, p. 1-31, Springer, New York.
[9] H. Xu, X. Mao, Q. Zheng, S. Wang, A-N Kawde, G. Liu, Anal. Chem. 81 (2009) 669–675.
[10] F. Sun, L. Liu, W. Ma, L.L Wang, C.L. Xu, H. Kuang, Int. J. Food Sci. Tech 47 (2012) 1505–1510.
[11] X. Mao, M. Baloda, A.S. Gurung, Y. Lin, G. Liu, Electrochem. Commun. 10 (2008) 1636–1640.
[12] H. Jans, Q. Huo, Chem. Soc. Rev. 41 (2012) 2849–2886.
[13] Diamond Electrochemistry, BKC-Elsevier, in: A. Fujishima, Y. Einaga, T.N. Rao, D.A. Tryk (Eds.), 2005.
[14] T.A. Ivandini, E. Saepudin, H. Wardah, N. Harmesa, Y. Dewangga, Einaga, Anal. Chem. 84 (2012) 9825–9832.
[15] L. Ouattara, I. Duo, T. Diaco, A. Ivandini, K. Honda, T. Rao, A. Fujishima, C. Comninellis, New Diam. Front. C. Tec 13 (2003) 97–108.
[16] O. El Tall, N. Jaffrezic-Renault, M. Sigaud, O. Vittori, Elecroanalysis 19 (2007) 1152–1159.
[17] Y. Nagaoka, T.A. Ivandini, D. Yamada, S. Fujita, M. Yamanuki, Y. Einaga, Chem. Lett 39 (2010) 1055–1057.
[18] L.A. Hutton, M.E. Newton, P.R. Unwin, J.V. Macpherson, Anal. Chem. 83 (2011) 735.
[19] A. Sugitani, T. Watanabe, T.A. Ivandini, T. Iguchi, Y. Einaga, Phys. Chem. Chem. Phys. 15 (2012) 142–147.
[20] C. Prado, S.J. Wilkins, F. Marken, R.G. Compton, Electroanalysis 14 (2002) 262–271.
[21] R.P. Subrayan, P.G. Rasmussen, Trends Polym. Sci. 3 (1995) 165–172.
[22] W.C. Andersen, S.B. Turnipseed, C.M. Karbiwnyk, S.B. Clark, M.R. Madson, C.M. Gieseker, R.A. Miller, N.G. Rummel, R. Reimschuessel, J. Agric. Food Chem. 56 (2008) 4340–4347.
[23] F. Sun, W. Ma, L. Xu, Y.Y. Zhu, L.Q. Liu, C.F. Peng, L.B. Wang, H. Kuang, C.L. Xu, Trac-Trend Anal. Chem 29 (2010) 1239–1249.
[24] C.A. Brown, K.-S. Jeong, R.H. Poppenga, B. Puschner, D.M. Miller, A.E. Ellis, K.-I. Kang, S. Sum, A.M. Cistola, S.A. Brown, J. Vet. Diagn. Invest. 19 (2007) 525–531.
[25] B. Puschner, R.H. Poppenga, L.J. Lowenstine, M.S. Filigenzi, P.A. Pesavento, J. Vet. Diagn. Invest. 19 (2007) 616–624.
[26] G. Liu, Y.Y. Lin, J. Wang, H. Wu, C.M. Wai, Y.H. Lin, Anal. Chem. 79 (2007) 7644–7653.
[27] K. Ushizawa, K. Watanabe, T. Ando, I. Sakaguchi, M. Nishitani-Gamo, Y. Sato, H. Kanda, Diam. Relat., Mater 7 (1998) 1719–1722.
[28] Y. Honda, T.A. Ivandini, T. Watanabe, K. Murata, Y. Einaga, Diam. Relat., Mater 40 (2013) 7–11.
[29] P.X. Zhao, N. Li, D. Astruc, Coord. Chem. Rev. 257 (2010) 638–665.
[30] R. Choico, S. Geoffrey, B. Eli, Immunology: A Short Course, John Wiley & Sons, 2003.
[31] M. Lintern, A. Mann, D. Longman, Anal. Chim. Acta 209 (1988) 193–203.
[32] M. Pourbaix, Atlas of Electrochemical Equilibria in Aqueous Solution, NACE Intl. Cebelcor, Houston, 1974.
[33] R. Uchikado, T.N. Rao, D.A. Tryk, A. Fujishima, Chem. Lett. 2 (2001) 144–145.
[34] T. Kondo, S. Aoshima, K. Honda, Y. Einaga, A. Fujishima, T. Kawai, J. Phys. Chem. C 111 (2007) 12650–12657.
[35] R.H. Tian, J.F. Zhi, Electrochem. Commun. 9 (2007) 1120–1126.
[36] T.A. Ivandini, Y. Naono, A. Nakajima, Y. Einaga, Chem. Let 34 (2005) 1086–1087.
[37] M.B. Gonzales-García, A. Costa-García, Bioelectroch. Bioener. 38 (1995) 389–395.
[38] A. Gillespie, D. Jao, A. Anriola, T. Dusa, C.F. Yang, L. Yu, Anal. Lett. 45 (2012) 1310–1320.
[39] M. Dequaire, C. Degrand, B. Limoges, Anal. Chem. 72 (2000) 5521–5528.
[40] D. Hernandez-Santoz, M.B. Gonzalez-Garcia, A. Costa-Garcia, J. Electroanal. Chem. 46 (2000) 607–615.
[41] L. Yu, A. Andriola, Talanta 28 (2010) 869–872.
[42] C. Terashima, T.N. Rao, B.V. Sarada, Y. Kubota, A. Fujishima, Anal. Chem. 75 (2003) 1564–1572.
[43] M. Chiku, T.A. Ivandini, A. Kamiya, A. Fujishima, Y. Einaga, J. Electroanal. Chem. 612 (2008) 201–207.
[44] X.M. Li, P.J. Luo, S.S. Tang, R.C. Beier, X.P. Wu, L.L. Yang, Y.W. Li, X.L. Xiao, J. Agric. Food. Chem. 59 (2011) 6064–6070.
[45] T. Le, P.F. Yan, J. Xu, Y.J. Hao, Food Chem. 138 (2013) 1610–1615.